Objective - Oriented Sequential Sampling for Simulation Based Robust Design Considering Multiple Sources of Uncertainty

Paul D. Arendt
Northwestern University, Department of Mechanical Engineering
2145 Sheridan Road Room B214
Evanston, IL, 60208
Phone: 847-491-5066, Fax: 847-491-3915, Email: paularendt2012@u.northwestern.edu

Daniel W. Apley
Northwestern University, Department of Industrial Engineering and Management Sciences
2145 Sheridan Road Room C150
Evanston, IL, 60208
Phone: 847-491-2397, Fax: 847-491-8005, Email: apley@northwestern.edu

Wei Chen*
*Corresponding Author
Northwestern University, Department of Mechanical Engineering
2145 Sheridan Road Room A216
Evanston, IL, 60208
Phone: 847-491-7019, Fax: 847-491-3915, Email: weichen@northwestern.edu

Abstract

Sequential sampling strategies have been developed for managing complexity when using computationally expensive computer simulations in engineering design. However, much of the literature has focused on objective-oriented sequential sampling methods for deterministic optimization. These methods cannot be directly applied to robust design which must account for uncontrollable variations in certain input variables (i.e., noise variables). Obtaining a robust design that is insensitive to variations in the noise variables is more challenging. Even though methods exist for sequential sampling in design under uncertainty, the majority of the existing literature does not systematically take into account the interpolation uncertainty that results from limitations on the number of simulation runs, the effect of which is inherently more severe than in deterministic design. In this paper, we develop a systematic objective-oriented sequential sampling approach to robust design with consideration of both noise variable uncertainty and interpolation uncertainty. The method uses Gaussian processes to model the costly simulator and quantify the interpolation uncertainty within a robust design objective. We examine several criteria, including our own proposed criteria, for sampling the design and noise variables and provide insight into their performance behaviors. We show that for both of the examples considered in this paper the proposed sequential algorithm is more efficient in finding the robust design solution than a one-shot space filling design.

Keywords: robust design, sequential sampling, metamodel, interpolation uncertainty

1 Introduction

To satisfy consumer expectations of high quality and low cost products, it is essential for a product design to be robust to the variations of uncertain input variables [1-3]. In simulation-based robust design, the computer simulation response is considered to be a function of two types of input variables – design ("control") variables and noise variables [1] – and the objective is to find a design that results in a desirable response mean and insensitivity or robustness to variation in the noise variables [1, 4].

Robust design formulations typically require a large number of simulations to directly determine statistical characteristics (e.g. mean and variance) of the response with respect to the distribution of the noise variables [5]. As computer simulations [4, 6] increase in accuracy (e.g., a finer mesh in FEA) and complexity, the computational cost of running extensive computer simulations becomes prohibitive. Global metamodels (a.k.a. surrogate models, emulators, response surface models, etc.) fitted over the design/noise variable input domain have generally been relied upon when searching for the optimal robust design [7, 8]. However, with limited sample sizes, the accuracy of such metamodels can be very poor. Metamodel accuracy relates to the ability of the metamodel to accurately interpolate between sampled simulation points, which Apley et al. [9] termed interpolation uncertainty. Furthermore, Jin et al. [10] have shown that interpolation uncertainty can have a large effect on robust design optimization.

Relative to the "one-shot" global metamodeling approach [11, 12], sequential sampling procedures can be more useful because they incorporate learning to ensure the maximum information is obtained from the fewest runs. They also allow the sample size to be determined adaptively as the data accumulates, which avoids conducting unnecessary additional computer simulations after a design is deemed sufficiently close to optimal. One form of sequential

sampling is objective-oriented sequential sampling [13-16], where one considers the specific manner in which the simulation results are to be used for optimizing a design objective. As depicted in Fig. 1 (for the deterministic optimization scenario in which the goal is to minimize the response y as a function of a design variable d, without any noise variables), in objective-oriented sequential sampling the goal is to select the next simulation point in a manner that balances between what appears to be a strong candidate for the optimal design (d_A), versus where interpolation uncertainty remains too large (d_B). As Jones et al. [13] and others have demonstrated, objective-oriented sequential sampling can provide an efficient means of arriving at the global optimum without producing a globally accurate metamodel of the computer simulator, which can result in tremendous computational savings over global metamodeling.

The aforementioned objective-oriented sequential sampling approaches have only been applied to deterministic optimization and cannot be directly applied to the optimization of a robust design objective function. In robust design, both noise and design variables must be selected in order to run the simulation, but the robust design objective function depends only on the design variables because the effects of the noise variables are integrated out (via Eq. (3), below) when calculating the performance mean and variation. Therefore, this body of work can only select the design variable setting and not the noise variable setting. Moreover, the adverse effects of interpolation uncertainty are compounded in robust design: Because the robust design objective function involves integration over a range of values for the noise variables, one cannot eliminate the effects of interpolation uncertainty with a single final confirmation run, as in deterministic optimization.

Previous authors [9, 17-19] quantified the interpolation uncertainty in the robust design objective based on a Bayesian analysis of a Gaussian process (GP) model (a.k.a. Gaussian

random process models) as the metamodel. Reference [9] considered an approach to reduce the impact of interpolation uncertainty by guiding users in selecting design variable sites for additional simulations based on graphical visualization of the effects of uncertainty on the robust design objective. However, [9] did not present a method for selecting the noise variable sites, nor did it present an automated algorithm for selecting design and/or noise sites. Furthermore, the graphical visualization techniques presented in [9] can be difficult to apply to high dimensional design applications. References [17-19] have adapted the expected improvement algorithm of [13] to robust design in the presence of noise variables. However, the robust design formulations used in their works include either the mean or the variance of the response in a robust design objective, but not both. Reference [20] used a robust design objective function that includes both the mean and variance, but the author does not systematically account for the effect of interpolation uncertainty on the robust design objective. Even though other methods for sequential sampling in design under uncertainty exist, these works focus on quantification of constraint response uncertainty in reliability-based design optimization using prediction intervals of response surface models [21, 22].

Unlike the informal graphical visualizations in [9] for additional computer simulations, in this paper we develop a systematic algorithmic sequential sampling method that is intended to efficiently identify the optimal robust design in the face of interpolation uncertainty. Like the approaches of [17-19], our approach considers both noise variable uncertainty and interpolation uncertainty and uses a Gaussian process framework to provide a consistent method of approximating the costly simulator and quantifying the resulting interpolation uncertainty. However, instead of considering only the mean or variance in the robust design objective, we develop an objective-oriented sequential sampling algorithm for a form of robust design in which

the single robust design objective function includes both the mean and the variance, the same objective function considered in [1, 8-10]. For many systems in which the response is of the smaller-is-better type, including both the mean and variance in the objective function constitutes a more natural robust design formulation than minimizing the variance under an inequality constraint on the mean, or vice-versa, as was done in [17].

Specifically, the contributions of this paper are to develop a formal systematic sequential sampling algorithm that (1) selects both the noise variable sites and the design variable sites, (2) optimally balances between reducing the effects of interpolation uncertainty versus sampling where the robust design objective function appears to be optimal, and (3) is applicable to a robust design objective function that considers both the mean and the standard deviation of the response. In Section 2, we review the approach for quantifying interpolation uncertainty in the robust design objective function. Next we introduce an illustrative example in Section 3 that we use throughout this paper to explain our proposed sequential sampling algorithm. In Section 4, we present our proposed objective-oriented sequential sampling algorithm and detail several different objective-oriented sampling criteria for selecting the simulation inputs in the robust design setting. In addition to the illustrative example introduced in Section 3, we apply the proposed sequential algorithm to the design of an automotive engine piston in Section 5. Both examples illustrate the effectiveness of the sequential sampling algorithm in efficiently finding the optimal robust design, and we also use them to assess the advantages and disadvantages of the competing criteria for determining the next sequentially sampled point. Section 6 concludes the paper.

2 Robust design with Gaussian process models

In this section, we briefly review the method for quantifying the effects of interpolation

uncertainty on the robust design objective function (see [9] for additional details). Let **d** denote a $n_d \times 1$ vector of design variables, **W** a $n_w \times 1$ vector of random noise variables, **w** a specific value for **W**, $p(\mathbf{w})$ the known probability distribution function of **W**, and $y(\mathbf{d},\mathbf{w})$ the response from a computationally expensive deterministic computer simulator as a function of **d** and **w**. By deterministic, we mean that the value of the response is exactly the same for repeated runs of the computer simulator at the same input settings for **d** and **w**.

The robust design objective that we consider is to find [1, 8, 10]

$$\mathbf{d}^* = \arg\min_{\mathbf{d}} \quad f(\mathbf{d}) \tag{1}$$

where $\mathbf{d}^*$ denotes the optimal robust design and the robust design objective function is

$$f(\mathbf{d}) = \mu(\mathbf{d}) + c\sigma(\mathbf{d}) \tag{2}$$

with c (e.g., c = 2, 3, etc.) denoting a user-defined constant that reflects risk attitude. The mean and variance of the response are

$$\begin{aligned} \mu(\mathbf{d}) &= E[y(\mathbf{d},\mathbf{W})] = \int y(\mathbf{d},\mathbf{w})\, p(\mathbf{w}) d\mathbf{w} \\ \sigma^2(\mathbf{d}) &= Var[y(\mathbf{d},\mathbf{W})] = \int [y(\mathbf{d},\mathbf{w}) - \mu(\mathbf{d})]^2\, p(\mathbf{w}) d\mathbf{w} \end{aligned} . \tag{3}$$

To consider the variation (e.g., manufacturing variation) in the design variables, one could decompose each uncertain design variable into one component that represents the nominal value of the design variable and a second component that represents the random error between the actual design variable and the nominal value [23]. For simplicity, in this paper we do not consider variation in the design variables, and we only consider the robust design objective function of Eq. (2) with no constraints.

Typically, the integrals of Eq. (3) require many evaluations of $y(\mathbf{d},\mathbf{w})$. To alleviate the associated computational burden, we create an easy to evaluate metamodel based on a smaller set of observations from $y(\mathbf{d},\mathbf{w})$. Then, instead of directly using $y(\mathbf{d},\mathbf{w})$, we use the prediction of the

metamodel over the domain of integration to approximate the mean and variance in Eq. (3). GP models are popular metamodels in the engineering and geostatistics community, with Kriging being one specific form of GP modeling [24-26]. GP models are ideal for representing deterministic computer simulations because they provide a prediction that passes exactly through every observation. Additionally, the GP model provides an inherent mechanism for quantifying the interpolation uncertainty at input points where no data has been observed. Other metamodeling techniques, e.g., radial basis functions [27], support vector regression [28], polynomial regression [29], etc., do not have an adequate mechanism for quantifying the interpolation uncertainty.

Adopting the same notation as [9], we use $G(\mathbf{d},\mathbf{w})$ to denote the GP model of the response, and we write the response as $Y(G,\mathbf{d},\mathbf{W}) = G(\mathbf{d},\mathbf{W})$. This allows us to express the response Y as a function $\mathbf{d}$ and of two random sources of uncertainty -- the interpolation uncertainty quantified by G and the uncertainty of the noise variables $\mathbf{W}$.

Likewise, we rewrite the robust design formulation of Eqs. (1), (2), and (3) as

$$\mathbf{d}^* = \arg\min_{\mathbf{d}} \quad F(\mathbf{d} \mid G) \tag{4}$$

where

$$F(\mathbf{d} \mid G) = \mu(\mathbf{d} \mid G) + c\sigma(\mathbf{d} \mid G) \tag{5}$$

with

$$\begin{aligned} \mu(\mathbf{d} \mid G) &= E[Y(G,\mathbf{d},\mathbf{W}) \mid G] = \int Y(G,\mathbf{d},\mathbf{w})\, p(\mathbf{w}) d\mathbf{w} \\ \sigma^2(\mathbf{d} \mid G) &= Var[Y(G,\mathbf{d},\mathbf{W}) \mid G] \\ &= \int [Y(G,\mathbf{d},\mathbf{w}) - \mu(\mathbf{d} \mid G)]^2\, p(\mathbf{w}) d\mathbf{w} \end{aligned} \quad . \tag{6}$$

An interpretation of this notational representation of the robust design objective function is as follows. In order to calculate Eqs. (2) and (3) directly, one must know the entire simulation

response surface $y(\mathbf{d},\mathbf{w})$, as opposed to just a set of observed simulated responses $\mathbf{y}^N = [y(\mathbf{d}_1,\mathbf{w}_1), \ldots, y(\mathbf{d}_N,\mathbf{w}_N)]$ at the input points $\{\mathbf{d}_i, \mathbf{w}_i: i = 1, \ldots, N\}$. But within the probabilistic GP framework, knowing the entire response surface corresponds to conditioning on G. Hence, Eqs. (4) – (6) are written as conditioned on G. Since we never know the entire response surface and must interpolate between simulated points, this also implies that we view $\mu(\mathbf{d}\,|\,G)$ and $\sigma^2(\mathbf{d}\,|\,G)$ as random variables via their dependence on the unknown complete response surface represented by the GP model G. In this respect, the notation $\mu(\mathbf{d}\,|\,G)$, $\sigma^2(\mathbf{d}\,|\,G)$, and $F(\mathbf{d}\,|\,G)$ indicates that the uncertainty in these quantities is due to having to interpolate the GP model of the response surface within the integrals of Eq. (6) at values other than the simulation points. Notice that this interpolation uncertainty is not due to variation in $\mathbf{W}$, because effects of the noise variables are integrated out in Eq. (6). In the remainder of this paper we refer to $F(\mathbf{d}\,|\,G)$ as the *stochastic robust design objective function*.

To quantify the interpolation uncertainty in $F(\mathbf{d}\,|\,G)$, [9] used the interval

$$F(\mathbf{d}\,|\,G) \in \mu_F(\mathbf{d}) \pm 2.0\sigma_F(\mathbf{d}) \tag{7}$$

which can be viewed as an approximate 95 % Bayesian prediction interval under the assumption that $F(\mathbf{d}\,|\,G)$ is approximately normally distributed. Here, $\mu_F(\mathbf{d})$ and $\sigma_F(\mathbf{d})$ denote the mean and standard deviation of $F(\mathbf{d}\,|\,G)$ (with respect to the posterior distribution of the random surface G, given the observed data $\mathbf{y}^N$) and are given by

$$\begin{aligned} \mu_F(\mathbf{d}) &= \mu_\mu(\mathbf{d}) + c\mu_\sigma(\mathbf{d}) \\ \sigma_F^2(\mathbf{d}) &= \sigma_\mu^2(\mathbf{d}) + c^2\sigma_\sigma^2(\mathbf{d}) + 2cCov[\mu(\mathbf{d}\,|\,G), \sigma(\mathbf{d}\,|\,G)] \end{aligned} \tag{8}$$

where

$$\begin{aligned} \mu_\mu(\mathbf{d}) &= E[\mu(\mathbf{d}\,|\,G)], \quad & \mu_\sigma(\mathbf{d}) &= E[\sigma(\mathbf{d}\,|\,G)] \\ \sigma_\mu^2(\mathbf{d}) &= Var[\mu(\mathbf{d}\,|\,G)], \quad & \sigma_\sigma^2(\mathbf{d}) &= Var[\sigma(\mathbf{d}\,|\,G)] \end{aligned}. \tag{9}$$

Equations for $\mu_\mu(\mathbf{d})$, $\mu_\sigma(\mathbf{d})$, $\sigma_\mu^2(\mathbf{d})$, $\sigma_\sigma^2(\mathbf{d})$, and $Cov[\mu(\mathbf{d}\,|\,G),\sigma(\mathbf{d}\,|\,G)]$ in terms of the GP model's posterior mean $\hat{y}(\mathbf{d},\mathbf{w}) = E[Y(G,\mathbf{d},\mathbf{w})\,|\,\mathbf{y}^N]$ and covariance $Cov[Y(G,\mathbf{d},\mathbf{w}),Y(G,\mathbf{d}',\mathbf{w}')\,|\,\mathbf{y}^N]$ are presented in Section 4 and in the appendix of [9]. Equations for the GP model's posterior mean and covariance are standard results [9, 24, 25] based on linear minimum mean square estimation or Bayesian analysis of linear Gaussian models and are presented in Appendix A of this paper.

The equations for $\mu_\mu(\mathbf{d})$, $\mu_\sigma(\mathbf{d})$, $\sigma_\mu^2(\mathbf{d})$, $\sigma_\sigma^2(\mathbf{d})$, and $Cov[\mu(\mathbf{d}\,|\,G),\sigma(\mathbf{d}\,|\,G)]$ require integration with respect to the noise variables, which can be implemented using numerical integration. Alternatively, in this paper we use closed form solutions for these integrals, which is possible if $p(\mathbf{w})$ is taken to be a multivariate normal distribution and the GP model uses a Gaussian correlation function with a constant prior mean. A prediction interval for $F(\mathbf{d}\,|\,G)$ of the form in Eq. (7) allows the designer to evaluate the impact of interpolation uncertainty on the robust design objective function, and it provides a basis for selecting points at which to run future simulations. One should note that $\sigma_F^2(\mathbf{d})$ in Eq. (8) is used to calculate $\sigma_F(\mathbf{d})$

As a side note, the value of $\sigma_F(\mathbf{d})$ directly quantifies the effect of interpolation uncertainty on the stochastic robust design objective function $F(\mathbf{d}\,|\,G)$. It should not be confused with $\sigma(\mathbf{d})$ of Eq. (2) , which represents the standard deviation of the response due to noise variable uncertainty, conditioned on knowing the entire response surface $G(\mathbf{d},\mathbf{w})$. The value of $\sigma_F(\mathbf{d})$ is not directly affected by noise variable uncertainty, since the noise variables have already been integrated out prior to Eqs. (8) and (9).

3 An Illustrative Example

In this section, we introduce an illustrative example, which is the same example

presented in [9]. The example involves designing an open box container to ferry a specified amount of gravel across a river. The response is the cost of the open box $y(d,W) = 80d^{-2} + 2dW + d^2W$ (modified from [30]), where the scalar design variable d represents the length of the bottom of the square box in meters with a range of [0.8, 2.5] m, and the scalar noise variable W represents the material cost per unit with a range of [7, 13] \$/m^2. To represent the uncertainty of the material cost, we assign a normal distribution to the noise variable $W \sim N(\mu_w, \sigma_w^2)$, with mean μ_w = 10 \$/m^2 and variance σ_w^2 = 2 \$^{2}/m^4. Although the response function is known and easy to evaluate, for illustrative purposes we treat it as a computationally expensive computer simulator.

Fig. 2 shows the response surface $y(d,w)$ and the resulting true robust design objective function from Eq. (2) with the optimal robust design of d^* = 1.34 m, for which $f(d^*)$ = \$108.30. The goal of our proposed sequential algorithm is to obtain d^*, and the associated $f(d^*)$, with the fewest number of computer simulator evaluations.

4 The proposed sequential sampling algorithm

The sequential sampling algorithm begins with an initial set of observations from the computer simulator and then sequentially determines the additional input settings (**d** and **w** both) at which to simulate the response in order to most efficiently find the optimal robust design. Fig. 3 is a flowchart for our proposed sequential sampling algorithm. In Fig. 3, the iteration number of the sequential algorithm is denoted by i and the data sequentially collected from the computer simulator is denoted by $\mathbf{y}^{N+i} = [y(\mathbf{d}_1,\mathbf{w}_1), \ldots, y(\mathbf{d}_{N+i},\mathbf{w}_{N+i})]$, where N is the size of the initial data set and $\{\mathbf{d}_{N+i}, \mathbf{w}_{N+i}\}$ are the next settings for the design variables and noise variables. The following subsections give details on the individual steps.

Although **d** and **w** are treated the same in the simulation (both as inputs), they have

completely different physical meaning, which must be taken into account when selecting the simulation points. Specifically, the robust design objective function depends explicitly on only **d**, but not on the noise variables, which are integrated out. Hence, although $\mathbf{d}_{N+i}$ can be chosen based on some appropriate measure of improvement in the objective function, $\mathbf{w}_{N+i}$ must be chosen differently. Intuitively, our criterion for choosing $\mathbf{w}_{N+i}$ is to minimize some measure of the impact of interpolation uncertainty on the robust design objective function. This idea of treating design variables and noise variables separately is similar to the method used in [16-20].

4.1 Step 0: Initial data set $\mathbf{y}^N$

The preliminary step of the algorithm is to gather an initial data set. Many authors suggest a space-filling experimental design, e.g. an optimal Latin hypercube design [16-19, 25, 31]. We too use an initial design of a 'maximin' optimal Latin hypercube (lhsdesign function in MATLAB®) [11] as the initial design. For sequential sampling, previous literature does not have a well-defined rule for the number of initial observations. We suggest $N \leq 10k$ [13], where k is the dimension of all the inputs (i.e., the dimension of **d** plus the dimension of **w**). One should also consider the available computational resources when determining the initial number of observations. In the open box example above, we began by observing four samples ($N = 4$) as shown in Fig. 4 "*Step 0: Initial data* ($\mathbf{y}^4$)". The iteration number i is set as 0. Fig. 4 will be used in the following subsections to illustrate the first iteration of the sequential sampling algorithm.

4.2 Step 1: Fit a GP model using $\mathbf{y}^{N+i}$

The first (iterative) step of the algorithm is to fit a GP model to the observed responses at the simulation points. Before fitting the GP model, we typically normalize the inputs of the simulator (the elements of **d** and **w**) to the range of 0 to 1 and standardize the output $\mathbf{y}^{N+i}$ to have a sample mean of 0 and a sample standard deviation of 1 [19, 32]. Then the parameters of the GP

model are estimated by using the maximum likelihood method (see [26] for details). "*Step 1: Fit GP model*" in Fig. 4 shows the posterior mean for the prediction of the GP model fitted to the 4 initial samples from Step 0. Set the iteration number to $i = i + 1$.

4.3 Step 2: Find $\mathbf{d}_{min}$ by minimizing the robust design objective function

After fitting the GP model to $\mathbf{y}^{N+i}$, we find the current best design by minimizing the robust design objective function that considers both the variability due to the random noise variables and the interpolation uncertainty. In analogy with Eq. (2), this robust design objective function is defined as

$$f_{GW}(\mathbf{d}) = E[Y(G,\mathbf{d},\mathbf{W})] + c\sqrt{Var[Y(G,\mathbf{d},\mathbf{W})}} \tag{10}$$

where the mean $E[Y(G,\mathbf{d},\mathbf{W})]$ and variance $Var[Y(G,\mathbf{d},\mathbf{W})]$ are with respect to both sources of uncertainty (c is the same user-defined constant as in Eq. (2)). The current best robust design $\mathbf{d}_{min}$ is defined as the minimizer of the robust design objective function in Eq. (10). Derivations for the mean and variance in Eq. (10) are presented in the Appendix B. The robust design objective function of Eq. (10) is a deterministic quantity because the mean and the variance account for all of the uncertainty. One should note that $F(\mathbf{d}\,|\,G)$ [defined in Eq. (5)] cannot be used as the objective function in this step because it is an unknown random quantity, due to its dependence on the unknown full response surface $G(\mathbf{d},\mathbf{w})$.

"*Step 2: Find* d_{min}" in Fig. 4 shows the robust design objective function from Eq. (10) using the GP model from the previous step for the open box example. One should notice that $f_{GW}(d)$ in Fig. 4 is much different in shape and magnitude as compared to $f(d)$ in Fig. 2(b), which is the result of the inaccuracy and large interpolation uncertainty of the GP model created based on the small initial data set. Note that $f_{GW}(d)$ in Fig. 4 does vary with respect to d, although it is difficult to discern from the axis scaling used in the figure.

4.4 Step 3: Find the next design variable setting $\mathbf{d}_{N+i}$

After finding $\mathbf{d}_{min}$, we select the next design variable setting $\mathbf{d}_{N+i}$ to balance between improving the robust design objective and reducing the uncertainty of the stochastic robust design objective function of Eq. (5) (i.e., the interpolation uncertainty). In this subsection, we use the confidence interval of the stochastic robust design objective function, discussed in Section 2, to determine the $\mathbf{d}_{N+i}$ that provides the best balance between improving the robust design and reducing the interpolation uncertainty. The idea here is similar to the traditional objective-oriented sequential sampling approach for deterministic optimization [13, 14], except that the deterministic objective response is now replaced by the stochastic robust design objective function.

We begin by adapting the expected improvement (EI) criterion [13, 14] to the stochastic robust design objective function. The original EI criterion has been shown in deterministic design to choose additional computer simulation points that balance the objective of improving the design while considering the reduction in interpolation uncertainty[13, 14]. To adapt EI to robust design, we define the improvement function to be (similar to [16-19])

$$I(\mathbf{d}) = \max(\mu_F(\mathbf{d}_{min}) - F(\mathbf{d} \mid G), 0) . \tag{11}$$

The improvement function quantifies the improvement of $F(\mathbf{d} \mid G)$ at the proposed design point $\mathbf{d}$ compared to $\mu_F(\mathbf{d}_{min})$ (the mean of the stochastic robust design objective function at $\mathbf{d}_{min}$). Since $\mu_F(\mathbf{d}_{min})$ is a deterministic quantity and $F(\mathbf{d} \mid G)$ is approximately normally distributed with a mean $\mu_F(\mathbf{d})$ and standard deviation $\sigma_F(\mathbf{d})$, the expectation of Eq. (11), termed the expected improvement, can be derived as (from [13, 14])

$$E[I(\mathbf{d})] = (\mu_F(\mathbf{d}_{min}) - \mu_F(\mathbf{d}))\Phi\left(\frac{\mu_F(\mathbf{d}_{min}) - \mu_F(\mathbf{d})}{\sigma_F(\mathbf{d})}\right) + \sigma_F(\mathbf{d})\phi\left(\frac{\mu_F(\mathbf{d}_{min}) - \mu_F(\mathbf{d})}{\sigma_F(\mathbf{d})}\right) \tag{12}$$

where $\Phi(\bullet)$ is the standard normal cumulative distribution function and $\phi(\bullet)$ is the standard normal probability distribution function. $\mathbf{d}_{N+i}$ is then selected as the value of $\mathbf{d}$ that maximizes the expected improvement. This is illustrated in Fig. 4 as "*Step 3: Find* d_5".

As an alternative to the EI criterion, we also propose the following prediction interval (PI) criterion to select $\mathbf{d}_{N+i}$. For the PI criterion, we select $\mathbf{d}_{N+i}$ to maximize the upper boundary of an approximate prediction interval for the potential improvement function $\mu_F(\mathbf{d}_{min}) - F(\mathbf{d} \mid G)$, which is

$$PI(\mathbf{d}) = \mu_F(\mathbf{d}_{min}) - \mu_F(\mathbf{d}) + z_p \sigma_F(\mathbf{d}) \tag{13}$$

where z_p denotes the $1 - p$ quantile of the standard normal distribution, and $\mu_F(\mathbf{d})$ and $\sigma_F(\mathbf{d})$ denote the mean and standard deviation of $F(\mathbf{d} \mid G)$. Eq. (13) assumes $F(\mathbf{d} \mid G)$ is approximately normally distributed. For the examples in this paper we use z_p = 3.0, which corresponds to a confidence level of 99.87%. Since Eq. (13) measures the extent to which the design $\mathbf{d}$ might potentially be better than the current optimal design $\mathbf{d}_{min}$ (with confidence $1 - p$), it inherently balances between sampling where the design appears to be a strong candidate for optimality, i.e. a high value of $\mu_F(\mathbf{d}_{min}) - \mu_F(\mathbf{d})$, versus where interpolation uncertainty is large, i.e. a high value for $\sigma_F(\mathbf{d})$. We evaluate and compare the EI and PI criteria in Section 5.

4.5 Step 4: Stopping criterion

After choosing $\mathbf{d}_{N+i}$, but before choosing $\mathbf{w}_{N+i}$, we assess a stopping criterion to determine whether the entire sequential algorithm should be terminated. In practice, the designer could set a limit on the number of computer simulations that are possible. In lieu of this, since the EI and PI criteria measure the potential improvement of design $\mathbf{d}_{N+i}$ compared to $\mathbf{d}_{min}$, another option is to stop the algorithm when either criterion indicates there is little potential for further improvement.

Because the criteria do not always decrease monotonically from one iteration to the next, the sequential algorithm can be stopped when the average of the criterion, over a specified number of previous iterations, is below a user specified value (see [17-19] for more details on algorithm termination using EI). A third alternative is to terminate the algorithm if the value of $\mathbf{d}_{min}$ does not change over several iterations, even if there still is substantial interpolation uncertainty. In this paper, we simply use a fixed number of iterations.

4.6 Step 5: Find the next noise variable setting $\mathbf{w}_{N+i}$

After selecting $\mathbf{d}_{N+i}$ and verifying that the stopping criteria is not satisfied, the next noise variable simulation point $\mathbf{w}_{N+i}$ is selected to achieve the greatest reduction in interpolation uncertainty. Several different criteria are defined below.

The simplest criterion for reducing interpolation uncertainty is perhaps to select $\mathbf{w}_{N+i}$ at the location where the uncertainty in the GP model is the largest [25], by maximizing the expression

$$MSE(\mathbf{w})s(\mathbf{w}) \tag{14}$$

where $MSE(\mathbf{w})$ is the mean squared error (MSE) of the GP model prediction, i.e. the posterior covariance of the GP model $Cov[Y(G,\mathbf{d}_{N+i},\mathbf{w}),Y(G,\mathbf{d}_{N+i},\mathbf{w})\,|\,\mathbf{y}^{N+i-1}]$ given the observed data $\mathbf{y}^{N+i-1}$, and $s(\mathbf{w})$ is some weight function. In [25], the weight function is taken to be a constant over the range of $\mathbf{w}$. Alternatively, [20] takes $s(\mathbf{w})$ to be the probability distribution of $\mathbf{w}$, i.e. $s(\mathbf{w}) = p(\mathbf{w})$. This weighted MSE function encourages the selection of $\mathbf{w}_{N+i}$ at noise locations that have higher probability of occurring. Using the constant weight function, this step is illustrated in Fig. 4 as "*Step 5: Find* w_5".

Another method to obtain the greatest reduction of interpolation uncertainty using the GP model is to select $\mathbf{w}_{N+i}$ at the minimum of the integrated mean squared error (IMSE). The IMSE

is defined as [25]

$$IMSE(\mathbf{w}) = \int MSE'(\mathbf{w}.\mathbf{w}')\, p(\mathbf{w}')d\mathbf{w}' \tag{15}$$

where the $MSE'(\mathbf{w},\mathbf{w}')$ is the posterior covariance of the GP model, which is

$$Cov[Y(G,\mathbf{d}_{N+i},\mathbf{w}'), Y(G,\mathbf{d}_{N+i},\mathbf{w}') \,|\, \mathbf{y}^{N+i-1}, y(\mathbf{d}_{N+i},\mathbf{w})]. \tag{16}$$

We note that Eq. (16) can be calculated prior to actually observing $y(\mathbf{d}_{N+i},\mathbf{w})$ [25]. By minimizing the IMSE, we are essentially selecting $\mathbf{w}_{N+i}$ at the point that minimizes the interpolation uncertainty over the entire domain of $\mathbf{w}$ at $\mathbf{d}_{N+i}$.

Another approach to select $\mathbf{w}_{N+i}$ is to reduce interpolation uncertainty by minimizing the expected value of the variance of the stochastic robust design function [18, 19]

$$E\left[Var[F(\mathbf{d}\,|\,G)\,|\,\mathbf{y}^{N+i-1}, y(\mathbf{d}_{N+i},\mathbf{w})]\,|\,\mathbf{y}^{N+i-1}\right]. \tag{17}$$

Since we have not observed the response at $\mathbf{d}_{N+i}$ and $\mathbf{w}$, the expectation in Eq. (17) is with respect to $y(\mathbf{d}_{N+i},\mathbf{w})$, which is a random quantity with distribution defined by the existing GP model from Step 2. Moreover, $Var[F(\mathbf{d}\,|\,G)\,|\,\mathbf{y}^{N+i-1}, y(\mathbf{d}_{N+i},\mathbf{w})]$ in Eq. (17) is $\sigma_F^2(\mathbf{d}_{N+i})$ [Eq. (8)] based on the observed data $\mathbf{y}^{N+i-1}$ and $y(\mathbf{d}_{N+i},\mathbf{w})$. One should note that the calculation of Eq. (17) has a higher computational expense compared to [18, 19], which only use either the mean or the variance in the robust design objective function.

We refer to the four above criteria as the maximum MSE with a constant weight function (MSE), the maximum weighted MSE (wMSE), the minimum IMSE (IMSE), and the minimum of the expected variance (VAR), which we compare in the examples of Section 5

4.7 Step 6: Conduct simulation at $\{\mathbf{d}_{N+i}, \mathbf{w}_{N+i}\}$ and form $\mathbf{y}^{N+i}$

After determining both $\mathbf{d}_{N+i}$ and $\mathbf{w}_{N+i}$, we conduct the simulation $y(\mathbf{d}_{N+i},\mathbf{w}_{N+i})$. We then form the data set $\mathbf{y}^{N+i} = [\mathbf{y}^{N+i-1}\ y(_{N+i},\mathbf{w}_{N+i})]$. For the first iteration of the open box example, we show the location for the next simulation in Fig. 4 *"Step 6: Conduct next simulation at* $\{d_5,w_5\}$".

As shown in the flow chart of Fig. 3, Steps 1 through 6 are repeated for the selection of the subsequent samples from the computer simulator and the algorithm ends when a stopping criterion is satisfied. The results after multiple iterations for the open box example are provided in the next section.

5 Results and discussion

In this section, we investigate two examples to (1) assess if the proposed sequential algorithm works effectively and efficiently for locating the robust optimal design and (2) assess which criteria for selecting $\mathbf{d}_{N+i}$ and $\mathbf{w}_{N+i}$ are the best suited for robust design.

5.1 Open box example

We continue the open box example using the EI criterion to select d_{N+i} and the MSE criterion to select w_{N+i}. The sequential algorithm is run for 11 iterations, which results in a total of 15 observations from the computer simulator. To determine if d_{min} and $f_{GW}(d_{min})$ of the sequential sampling algorithm converges to d^* and $f(d^*)$, we plot d_{min} and $f_{GW}(d_{min})$ over the iterations of the algorithm in Fig. 5(a). Fig. 5(a) shows that d_{min} converges to d^* indicating that the sequential algorithm can find the optimal robust design. Furthermore, $f_{GW}(d_{min})$ converges to $f(d^*)$ indicating that the interpolation uncertainty of the robust design objective function $f_{GW}(d)$ in the neighborhood of d^* is small. To further illustrate the behavior of the sequential sampling algorithm, the locations of the 11 sequentially added observations are shown in Fig. 5(b). As the algorithm progresses, the samples initially explore the design variable space and eventually congregate in the neighborhood of d^* spanning the range of w. The relatively large number of points in the neighborhood of d^* decreases the interpolation uncertainty in this region, and thus $f_{GW}(d_{min})$ can converge to $f(d^*)$.

Next we continue the open box example to explore the different combinations of the

criteria for selecting d_{N+i} and w_{N+i} (Sections 4.4 and 4.6). Recall that the EI and PI criteria are for selecting d_{N+i}, and the MSE, wMSE, IMSE, and VAR criteria are for selecting w_{N+i}. We ran the sequential algorithm for the remaining seven possible combinations of two types of criteria using the same number of iterations and initial data points as above. Table 1 reports d_{min} and $f_{GW}(d_{min})$, for the eight combinations of criteria, along with the true optimal robust design. To quantify the interpolation uncertainty at d_{min}, Table 1 also reports $\sigma_F(d_{min})$. As a final check of the accuracy of the stochastic robust design objective function, we also report the value of $f(d_{min})$.

All of the combinations of criteria accurately identified d^* with similar results. One should note that when using the VAR criterion to select w_{N+i} the resulting $\sigma_F(d_{min})$ was larger compared to the other combinations, which indicates the combinations with VAR had more interpolation uncertainty at d_{min}. We also found the VAR criterion tends to select w_{N+i} extremely close to previously sampled points, which is a result of numerical instabilities in calculating Eq. (17). Moreover, as noted by [31], the VAR criterion is computationally expensive. Therefore, we recommend not to use the VAR criterion to select w_{N+i}, and we do not further consider it in this paper.

Although similar results are obtained for the six combinations of the criteria, one should note that the selection criterion for w_{N+i} significantly affects where the locations for w are chosen. For instance, the IMSE and wMSE criteria select points on the interior of the domain of w, whereas the MSE criterion tends to select points on the boundary of the domain of w. This observation is consistent with the previous literature [16, 20, 25].

Also included in Table 1 are two one-shot scenarios, as a comparison to the sequential algorithm. Both one-shot scenarios collected 15 computer simulations evenly spread over the domain of d and w (using a 'maximin' optimal Latin hypercube design). The first scenario "One-

shot (IU)" has the same robust design objective function of Eq. (10), which considers both the variation of the noise variables and the interpolation uncertainty (IU). In the second scenario "One-shot (no IU)" the objective function is the same as Eq. (2), except the mean and variance of Eq. (3) are calculated by substituting the posterior mean of the GP model in place of the true response function $y(d,w)$. This second scenario neglects the interpolation uncertainty when finding the optimal robust design and is more widely used because it is simpler to implement [10]. In order to achieve a fair comparison between the results of the sequential sampling algorithm and the results of the "One-shot (no IU)" scenario, for the "One-shot (no IU)" scenario in Table 1 we report the values of $f_{GW}(d_{\min})$ given that d_{min} was found using the objective function of the "One-shot (no IU)" scenario. Since optimal Latin hypercube designs are random, we repeated the one-shot analyses for 30 different optimal Latin hypercube designs, and the one-shot results in Table 1 are the averages over the 30 replicates. Since 15 data points are quite sufficient for this low dimensional problem in creating a GP model with very little interpolation uncertainty, both one-shot scenarios produce similar results. Additionally, both one-shot scenarios provide an accurate value for the optimal robust design d^* similar to the sequential algorithm using the different combinations of criteria, with the exception of VAR (which we do not recommend). However, the sequential algorithm produces a smaller value of $\sigma_F(d_{min})$ compared to both one-shot scenarios. Smaller values of $\sigma_F(d_{min})$ indicate that the sequential algorithm is more effective at minimizing the interpolation uncertainty compared to the one-shot scenarios.

This is consistent with Fig. 5(a), which shows that the sequential algorithm converged to the optimal robust design after only seven iterations (for a total of 11 simulation points). In contrast, the results for the one-shot experiments with 11 simulation points are inferior ("One-

shot (IU)" $f_{GW}(d_{min})$ had a mean of \$109.02 with maximum of \$137.15 and minimum of \$104.23, and "One-shot (no IU)" $f_{GW}(d_{min})$ had a mean of \$107.62 with a maximum of \$108.75 and minimum of \$107.32). Although the differences between the one-shot and sequential designs are relatively small in this low-dimensional example with a smooth response surface, in the next section the differences are more pronounced for the design of an automotive engine piston example with 4 design variables and 2 noise variables.

5.2 Piston Design Example

In this section, we demonstrate the general application of the proposed sequential sampling algorithm with the design of an automotive engine piston that was previously analyzed in [9, 33]. Since engine noise is one of the key factors in customer dissatisfaction, the objective is to obtain a design that minimizes the piston slap noise and is invariant to the noise variables. Piston slap noise is the engine noise that results from the secondary motion of the piston. To simulate the piston slap noise, [6] developed a computationally intensive simulation model using multi-body dynamics. The response y from this computer simulator is defined as the sound power level of the piston slap noise. Table 2 contains the descriptions of the four design variables and the two noise variables. The design variables control the geometry of the piston, whereas the uncertainty in the noise variables is caused by variation in environmental conditions, e.g., temperature, wear, and spark timing.

Due to the high computational expense of the multi-body computer simulation, the true response surface for the piston design example is unknown. Therefore, in order to gauge the effectiveness of the proposed sequential sampling algorithm, we take the same approach as [9] and build a GP model based on a relatively large and evenly spaced data set of 200 samples observed directly from the multi-body computer simulator. Then the posterior mean of this large

GP model is treated as the "true" response surface. This yields the true optimal robust design as $\mathbf{d}^* = [2.325\ 1.300\ 25.000\ 1.000]^T$ and $f(\mathbf{d}^*) = 53.82$.

We now apply the sequential sampling algorithm as described in Section 4, where the easy-to-compute "true" response surface is the posterior mean of the large GP model (based on the 200 simulations). The initial design is a 10 point 'maximin' optimal Latin hypercube design. Then the sequential algorithm was run for 20 iterations (providing a total of 30 observations). In light of the similar results for the different sequential algorithms for the open box example, we only considered the PI criterion to select $\mathbf{d}_{N+i}$ and the wMSE criterion to select $\mathbf{w}_{N+i}$ in this example.

As with the previous example, we compare the results from the sequential sampling algorithm to the results from one-shot scenarios, "One-shot (IU)" and "One-shot (no IU)". For each one-shot scenario, we ran 30 different 'maximin' Latin hypercube designs. To compare the convergence behavior, Fig. 6 plots $f_{GW}(\mathbf{d}_{min})$ of the sequential algorithm verses the iteration number. Fig. 6 also plots the average $f_{GW}(\mathbf{d})$ across the 30 replicates (each with a different Latin hypercube design) for both one-shot scenarios, with the error bars indicating the maximum and minimum values over the 30 replicates. Similar to the previous example, for the "One-shot (no IU)" scenario in Fig. 6 we plot $f_{GW}(\mathbf{d}_{min})$ given that $\mathbf{d}_{min}$ is obtained from an objective function that neglects the interpolation uncertainty. Comparing the two one-shot scenarios, Fig. 6 shows they have similar convergence behavior for the mean, and their error bars generally decrease as more points are added. For the "One-shot (no IU)", a small error bar at $i = 0$ was observed, which is a result of this scenario neglecting interpolation uncertainty and consistently obtaining $\mathbf{d}_{min}$ values in regions with large amounts of interpolation uncertainty. These large amounts of interpolation uncertainty resulted in $f_{GW}(\mathbf{d}_{min})$ being consistently large. Comparing the one-shot

scenarios to the sequential algorithm, from Fig. 6 we see that as the iterations increases the sequential algorithm converges faster to the optimal robust design. For example, if we stopped the sequential algorithm at $i = 15$, then the results for the sequential algorithm are superior to the results of both one-shot scenarios. Additionally, for lower numbers of sample points (e.g., $i \leq 5$), both the one-shot scenarios and the sequential algorithm have a value of $f_{GW}(\mathbf{d}_{min})$ much larger than $f(\mathbf{d}^*)$ because neither have enough information about the response.

Although we omit the results for brevity, we also observed that the sequential sampling algorithm obtained a much smaller value of $\sigma_F(\mathbf{d}_{min})$ than both of the one-shot scenarios, similar to what was observed in Table 1 for the open box example. The smaller value indicates that the sequential algorithm effectively decreased the interpolation uncertainty at $\mathbf{d}_{min}$. Thus, in this example, we showed that (1) the sequential sampling algorithm can be applied to higher dimensional engineering applications and (2) the sequential sampling algorithm accurately identifies the optimal robust design with greater efficiency and less interpolation uncertainty than the one-shot designs.

6 Conclusions

The majority of previous literature using objective-oriented sequential sampling approaches has focused on global optimization of deterministic functions. In this paper, we have developed an objective-oriented sequential sampling algorithm for robust design considering noise variable uncertainty together with interpolation uncertainty. Because of the uncertainty in the noise variables, the effects of interpolation uncertainty on the robust design objective function are far less transparent than its effects on a deterministic objective.

As illustrated in two examples, our sequential algorithm obtained an optimal robust

design with a small number of observations from the computer simulator. Additionally, we also explored several different criteria for the selection of both the design variables and the noise variables. For selecting the next design variable setting, both the EI criterion and PI criterion efficiently identified the optimal robust design. When selecting the noise variable setting, the IMSE and wMSE criteria reduced the interpolation uncertainty more efficiently than the MSE and VAR criteria. Therefore, we suggest implementing the sequential algorithm using the EI or PI criteria for selecting the design variables and the wMSE or IMSE criteria for selecting the noise variables.

The sequential algorithm presented in this paper can be applied to many different engineering applications involving computationally expensive physics-based computer models. This sequential algorithm helps an engineer to efficiently collect simulation data in order to obtain an optimal design that is insensitive to the variation of the noise variables, and therefore to design higher quality, higher reliability products in less time.

Although this research has addressed the problem of robust design when using computationally expensive simulators, future research is needed to apply the algorithm more effectively to many practical design problems, especially in high dimensions. Since many design scenarios involve constraints, the proposed sequential algorithm should be augmented to consider constraints. Additionally, our sequential algorithm can be computationally demanding due to the calculations for the mean and variance of the stochastic robust design objective function of Eq. (5). The computational cost of the sequential algorithm increases exponentially as the number of observations increases. For example, with 10 and 70 observations, one full iteration of our proposed sequential algorithm can require 30 seconds and 1.5 hours, respectively, of computation time (on a single Intel 2.66 GHz processor). However, we consider the proposed

sequential algorithm to be less computationally demanding than directly optimizing the expensive computer simulator. The computational efficiency and numerical stability of the proposed algorithm could potentially be improved by incorporating the most recent advances in Gaussian process models (for examples see [34, 35]). Finally, one could include additional sources of uncertainty into the sequential sampling algorithm (e.g., including the variation in the design variables as in [23]). Altogether, further research will enable the use of the proposed sequential algorithm for problems with higher dimensions and a larger number of observations.

7 Acknowledgements

The grant support from the National Science Foundation (CMMI-0928320, CMMI-0758557, and CMMI-1233403) is greatly acknowledged. The views expressed are those of the authors and do not necessarily reflect the views of the sponsors.

Nomenclature

$E[I(\mathbf{d})]$	Expected Improvement (EI) criterion at $\mathbf{d}$
$F(\mathbf{d} \mid G)$	The stochastic robust design objective function
$G(\mathbf{d},\mathbf{w})$, G	GP model of the response $y(\mathbf{d},\mathbf{w})$
$\mathbf{H}$	Regression functions matrix for the mean of a GP model
$I(\mathbf{d})$	The improvement function used in the EI criterion
$IMSE(\mathbf{w})$	The Integrated Mean Squared Error (IMSE) at $\mathbf{w}$
IU	Interpolation Uncertainty
$MSE(\mathbf{w})$	The Mean Squared Error (MSE) at $\mathbf{w}$
PI($\mathbf{d}$)	Prediction Interval (PI) criterion at $\mathbf{d}$
$R((\mathbf{d}, \mathbf{w}), (\mathbf{d}', \mathbf{w}'))$	Correlation function of a GP model between points ($\mathbf{d}$, $\mathbf{w}$) and ($\mathbf{d}'$, $\mathbf{w}'$)
$\mathbf{R}$	Correlation matrix of a GP model

$\mathbf{W}$	Vector of random noise variables ($n_w \times 1$)
wMSE	weighted Mean Squared Error
$Y(G,\mathbf{d},\mathbf{W})$	The response of $y(\mathbf{d},\mathbf{w})$ with both interpolation uncertainty and noise variable uncertainty
c	User-defined constant that reflects risk attitude
$\mathbf{d}$	Vector of design variables ($n_d \times 1$)
$\mathbf{d}^*$	The optimal robust design
$\mathbf{d}_{N+i}$	The next settings for the design variables
$\mathbf{d}_{min}$	The location of the minimum value of $f_{GW}(\mathbf{d})$
$f(\mathbf{d})$	Robust design objective function
$f_{GW}(\mathbf{d})$	Robust design objective function that includes both the interpolation uncertainty and the noise variable uncertainty
$\mathbf{h}(\mathbf{d},\mathbf{w})$	Vector of regression functions for the mean function of a GP model
i	Iteration number of the sequential sampling algorithm
$p(\mathbf{w})$	Known probability distribution function of $\mathbf{W}$
$s(\mathbf{w})$	Weight function used in the wMSE
$\mathbf{w}$	Represents a specific realization of $\mathbf{W}$
$\mathbf{w}_{N+i}$	The next settings for the noise variables
$y(\mathbf{d},\mathbf{w})$	The response from a computationally expensive deterministic computer simulator
$\mathbf{y}^N$	Observed data from the computer simulator ($N \times 1$)
$\mathbf{y}^{N+i}$	Collection of observed computer simulator data at iteration i
$\hat{y}(\mathbf{d},\mathbf{w})$	Mean prediction of the response based on the GP model
z_p	The 1 - p quantile of the standard normal distribution

$\boldsymbol{\beta}$ Regression coefficients for the mean function of a GP

$\mu(\mathbf{d})$ Mean of the response $y(\mathbf{d},\mathbf{W})$, which depends on the value $\mathbf{d}$

$\mu(\mathbf{d}\,|\,G)$ Mean of the response $Y(G,\mathbf{d},\mathbf{W})$

$\mu_F(\mathbf{d})$ Mean of $F(\mathbf{d}\,|\,G)$

$\mu_\mu(\mathbf{d})$ Expected value of $\mu(\mathbf{d}\,|\,G)$

$\mu_\sigma(\mathbf{d})$ Expected value of $\sigma(\mathbf{d}\,|\,G)$

$E\left[Var[F(\mathbf{d}\,|\,G)\,|\,\mathbf{y}^{N+i-1}, y(\mathbf{d}_{N+i},\mathbf{w})]\,|\,\mathbf{y}^{N+i-1}\right]$ Expected value of $\sigma_F^2(\mathbf{d}_{N+i})$ (VAR) based on the observed data from the computer simulator $\mathbf{y}^{N+i-1}$ and the next computer simulation $y(\mathbf{d}_{N+i},\mathbf{w})$

σ^2 Constant variance of the GP model

$\sigma^2(\mathbf{d}), \sigma(\mathbf{d})$ Variance and standard deviation of the response $y(\mathbf{d},\mathbf{W})$, which depends on $\mathbf{d}$

$\sigma^2(\mathbf{d}\,|\,G), \sigma(\mathbf{d}\,|\,G)$ Variance and standard deviation of the response $Y(G,\mathbf{d},\mathbf{W})$

$\sigma_F^2(\mathbf{d})$, $\sigma_F(\mathbf{d})$ Variance and standard deviation of $F(\mathbf{d}\,|\,G)$

$\sigma_\mu^2(\mathbf{d})$ Variance of $\mu(\mathbf{d}\,|\,G)$

$\sigma_\sigma^2(\mathbf{d})$ Variance of $\sigma(\mathbf{d}\,|\,G)$

$\boldsymbol{\omega}$ Roughness parameters for the correlation function of a GP model

Appendix A: Gaussian process model Posterior mean and covariance

In this appendix we briefly review the Bayesian analysis of a GP model (see [9] for more details). To begin, in the GP model approach one assumes the response $y(\mathbf{d},\mathbf{w})$ is a single realization of a spatial random process with prior mean $\mathbf{h}(\mathbf{d},\mathbf{w})\boldsymbol{\beta}$, where $\mathbf{h}(\mathbf{d},\mathbf{w})$ is a row vector of regression functions (here we assume $\mathbf{h}(\mathbf{d},\mathbf{w}) = 1$) and $\boldsymbol{\beta}$ is a column vector of regression coefficients, and prior covariance of $\sigma^2 R((\mathbf{d},\mathbf{w}),(\mathbf{d}',\mathbf{w}'))$, where σ^2 is a constant and

$R((\mathbf{d},\mathbf{w}),(\mathbf{d}',\mathbf{w}'))$ is a Gaussian correlation function between the responses observed at $(\mathbf{d},\mathbf{w})$ and $(\mathbf{d}',\mathbf{w}')$. The Gaussian correlation function takes the form of

$$R((\mathbf{d},\mathbf{w}),(\mathbf{d}',\mathbf{w}')) = \prod_{i=1}^{n_d} \exp\{\omega_i (\mathbf{d}_i - \mathbf{d}'_i)^2\} \prod_{j=1}^{n_w} \exp\{\omega_{n_d+j} (\mathbf{w}_j - \mathbf{w}'_j)^2\} \tag{18}$$

where $\boldsymbol{\omega}$ is a vector of roughness parameters.

After observing the computer simulations $\mathbf{y}^N$ at the input points $\{\mathbf{d}_i, \mathbf{w}_i: i = 1, \ldots, N\}$, the posterior distribution of the GP model for the response is Gaussian with a mean and covariance of (and given $\boldsymbol{\omega}$ and σ^2 with a non-informative prior for $\boldsymbol{\beta}$) [36]

$$\begin{aligned} E[y(\mathbf{d},\mathbf{w}) \mid \mathbf{y}^N] &= E[Y(G,\mathbf{d},\mathbf{w})] \\ &= \mathbf{h}(\mathbf{d},\mathbf{w})\hat{\boldsymbol{\beta}} + \mathbf{r}^T(\mathbf{d},\mathbf{w})\mathbf{R}^{-1}(\mathbf{y}^N - \mathbf{H}\hat{\boldsymbol{\beta}}) \\ &= \hat{y}(d,w) \end{aligned} \tag{19}$$

$$\begin{aligned} Cov[y(\mathbf{d},\mathbf{w}), y(\mathbf{d}',\mathbf{w}') \mid \mathbf{y}^N] &= Cov[Y(G,\mathbf{d},\mathbf{w}), Y(G,\mathbf{d}',\mathbf{w}') \mid \mathbf{y}^N] \\ &= \sigma^2\{R((\mathbf{d},\mathbf{w}),(\mathbf{d}',\mathbf{w}') - \mathbf{r}^T(\mathbf{d},\mathbf{w})\mathbf{R}^{-1}\mathbf{r}(\mathbf{d}',\mathbf{w}') \\ &\quad + (\mathbf{h}(\mathbf{d},\mathbf{w})^T - \mathbf{H}^T\mathbf{R}^{-1}\mathbf{r}(\mathbf{d},\mathbf{w}))^T(\mathbf{H}^T\mathbf{R}^{-1}\mathbf{H})^{-1}(\mathbf{h}(\mathbf{d}',\mathbf{w}')^T - \mathbf{H}^T\mathbf{R}^{-1}\mathbf{r}(\mathbf{d}',\mathbf{w}'))\} \end{aligned} \tag{20}$$

where $\mathbf{r}(\mathbf{d},\mathbf{w})$ is a $N \times 1$ vector whose ith element is $R((\mathbf{d},\mathbf{w}),(\mathbf{d}_i,\mathbf{w}_i))$. $\mathbf{R}$ is a $N \times N$ matrix whose ith row and jth column element is $R((\mathbf{d}_i,\mathbf{w}_i),(\mathbf{d}_j,\mathbf{w}_j))$, $\mathbf{H}$ is a $N \times 1$ vector whose ith element is $\mathbf{h}(\mathbf{d}_i,\mathbf{w}_i)$, and $\hat{\boldsymbol{\beta}} = [\mathbf{H}^T\mathbf{R}^{-1}\mathbf{H}]^{-1}\mathbf{H}^T\mathbf{R}^{-1}\mathbf{y}^N$. In the case $\boldsymbol{\omega}$ and σ^2 are unknown, one usually estimates their values using the maximum likelihood method [26]. These maximum likelihood estimates for $\boldsymbol{\omega}$ and σ^2 are then plugged into Eqs. (19) and (20).

Appendix B: Mean and variance of the robust design objective function

The mean $E[Y(G,\mathbf{d},\mathbf{W})]$ and variance $Var[Y(G,\mathbf{d},\mathbf{W})]$, used in the robust design function of Eq. (10) can be derived in terms of the posterior distribution of the GP model. The derivation for the mean is

$$\begin{aligned} E[Y(G,\mathbf{d},\mathbf{W})] &= E[E[Y(G,\mathbf{d},\mathbf{W}) \mid \mathbf{W} = \mathbf{w}]] \\ &= E[\hat{y}(\mathbf{d},\mathbf{W})] \\ &= \mu_\mu(\mathbf{d}) \end{aligned} \quad . \tag{21}$$

In the first line of Eq. (21), the expectation $E[Y(G,\mathbf{d},\mathbf{W}) \mid \mathbf{W}=\mathbf{w}]$ is taken with respect to the posterior distribution of the GP model assuming a value of $\mathbf{w}$ for $\mathbf{W}$, and the outer expectation $E[\bullet]$ is with respect to the noise variables $\mathbf{W}$. Using a similar notation, the variance $Var[Y(G,\mathbf{d},\mathbf{W})]$ can be derived as

$$Var[Y(G,\mathbf{d},\mathbf{W})] = E[Var[Y(G,\mathbf{d},\mathbf{W}) \mid G]] + Var[E[Y(G,\mathbf{d},\mathbf{W}) \mid G]], \tag{22}$$

which is a result of the law of total variance [37]. The $Var[Y(G,\mathbf{d},\mathbf{W}) \mid G]$ and $E[Y(G,\mathbf{d},\mathbf{W}) \mid G]$ are with respect to the noise variable and the outer $E[\bullet]$ and $Var[\bullet]$ are with respect to the posterior of the GP model. Using the notation in [9], we can rewrite $Var[Y(G,\mathbf{d},\mathbf{W})]$ as

$$Var[Y(G,\mathbf{d},\mathbf{W})] = \mu_S(\mathbf{d}) + \sigma_\mu^2(\mathbf{d}). \tag{23}$$

where $\mu_S(\mathbf{d}) = E[Var[Y(G,\mathbf{d},\mathbf{W}) \mid G]]$ and $\sigma_\mu^2(\mathbf{d}) = Var[E[Y(G,\mathbf{d},\mathbf{W}) \mid G]]$. Detailed equations for $\mu_\mu(\mathbf{d})$, $\mu_S(\mathbf{d})$, and $\sigma_\mu^2(\mathbf{d})$ can be found in [9].

References

[1] Chen, W., Allen, J. K., Tsui, K.-L., and Mistree, F., 1996, "A Procedure for Robust Design: Minimizing Variations Caused by Noise Factors and Control Factors," Journal of Mechanical Design, 118(4), pp. 478-485.

[2] Al-Widyan, K., and Angeles, J., 2005, "A Model-Based Formulation of Robust Design," Journal of Mechanical Design, 127(3), pp. 388-396.

[3] Chang, P. B., Williams, B. J., Bhalla, K. S. B., Belknap, T. W., Santner, T. J., Notz, W. I., and Bartel, D. L., 2001, "Design and Analysis of Robust Total Joint Replacements: Finite Element Model Experiments with Environmental Variables," Journal of Biomechanical Engineering, 123(3), pp. 239-246.

[4] Youn, B. D., Choi, K. K., and Park, Y. H., 2003, "Hybrid Analysis Method for Reliability-Based Design Optimization," Journal of Mechanical Design, 125(2), pp. 221-232.

[5] Lee, S., and Chen, W., 2008, "A Comparative Study of Uncertainty Propagation Methods for Black-Box-Type Problems," Struct Multidisc Optim, 37(3), pp. 239-253.

[6] Hoffman, R., Sudjianto, A., Du, X., and Stout, J., 2003, "Robust Piston Design and Optimization Using Piston Secondary Motion Analysis," SAE Paper (Paper No. 2003-01-0148).

[7] Repalle, J., and Grandhi, R. V., 2005, "Design of Forging Process Variables under Uncertainties," Journal of Materials Engineering and Performance, 14(1), pp. 123-131.

[8] Aslett, R., Buck, R. J., Duvall, S. G., Sacks, J., and Welch, W. J., 1998, "Circuit Optimization Via Sequential Computer Experiments: Design of an Output Buffer," Journal of the Royal Statistical Society: Series C, 47(1), pp. 31-48.

[9] Apley, D., Liu, J., and Chen, W., 2006, "Understanding the Effects of Model Uncertainty in Robust Design with Computer Experiments," Journal of Mechanical Design, 128(4), pp. 945-958.

[10] Jin, R., Du, X., and Chen, W., 2003, "The Use of Metamodeling Techniques for Optimization under Uncertainty," Structural and Multidisciplinary Optimization, 25(2), pp. 99-116.

[11] Mckay, M. D., and Conover, W., 1979, "A Comparison of Three Methods for Selecting Values of Input Variables in the Analysis of Output from a Computer Code," Technometrics, 21(2), pp. 239-245.

[12] Osio, I., and Amon, C. H., 1996, "An Engineering Design Methodology with Multistage Bayesian Surrogates and Optimal Sampling " Research in Engineering Design, 8(4), pp. 189.

[13] Jones, D. R., Schonlau, M., and Welch, W. J., 1998, "Efficient Global Optimization of Expensive Black-Box Functions," Journal of Global Optimization, 13(4), pp. 455-492.

[14] Schonlau, M., Welch, W. J., and Jones, D. R., 1998, "Global Versus Local Search in Constrained Optimization of Computer Models," Lecture Notes-Monograph Series, 34, pp. 11-25.

[15] Picheny, V., Ginsbourger, D., Roustant, O., Haftka, R. T., and Kim, N.-H., 2010, "Adaptive Designs of Experiments for Accurate Approximation of a Target Region," Journal of Mechanical Design, 132(7), pp. 071008.

[16] Lam, C., 2008, "Sequential Adaptive Designs in Computer Experiments for Response Surface Model Fit," Ph.D. thesis, The Ohio State University, Columbus, OH.

[17] Lehman, J., Santner, T. J., and Notz, W., 2004, "Designing Computer Experiments to Determine Robust Control Variables," Statistica Sinica, 14(2), pp. 571-590.

[18] Williams, B. J., Santner, T. J., and Notz, W., 2000, "Sequential Design of Computer Experiments to Minimize Integrated Response Functions," Statistica Sinica, 10(4), pp. 1133-1152.

[19] Williams, B. J., Santner, T. J., Notz, W. I., and Lehman, J. S., 2010, *Statistical Modelling and Regression Structures*, Springer, Berlin, Germany, "Sequential Design of Computer Experiments for Constrained Optimization".

[20] Jurecka, F., 2007, "Robust Design Optimization Based on Metamodeling Techniques," Ph.D. thesis, Technical University of Munich, Munich, Germany.

[21] Kim, C., and Choi, K. K., 2008, "Reliability-Based Design Optimization Using Response Surface Method with Prediction Interval Estimation," Journal of Mechanical Design, 130(12), pp. 121401.

[22] Zhao, L., Choi, K. K., Lee, I., and Du, L., 2009, "Response Surface Method Using Sequential Sampling for Reliability-Based Design Optimization," ASME International Design Engineering Technical Conferences, Brooklyn, NY.

[23] Zhang, S., Zhu, P., Chen, W., and Arendt, P., 2012, "Concurrent Treatment of Parametric Uncertainty and Metamodeling Uncertainty in Robust Design," Structural and Multidisciplinary Optimization, pp. 1-14.

[24] O'hagan, A., 1978, "Curve Fitting and Optimal Design for Prediction," Journal of the Royal Statistical Society: Series B, 40(1), pp. 1-41.

[25] Sacks, J., Welch, W. J., Mitchell, T. J., and Wynn, H. P., 1989, "Design and Analysis of Computer Experiments," Statistical Science, 4), pp. 409-423.

[26] Schabenberger, O., and Gotway, C., 2005, *Statistical Methods for Spatial Data Analysis Text in Statistical Science*, Chapman & Hall/CRC, Boca Raton, Florida.

[27] Bushman, M., 2003, *Radial Basis Functions: Theory and Implementations*, Cambridge University Press, Cambridge, England.

[28] Vapnik, V., 2000, *The Nature of Statistical Learning*, Springer Science+Business Media, Berlin, Germany.

[29] Myers, R., and Montgomery, D., 2002, *Response Surface Methodology: Process and Product Optimization Using Designed Experiments*, John Wiley & Sons, Inc., Hoboken, NJ.

[30] Duffin, R., Peterson, E., and Zener, C., 1967, *Geometric Programming*, Wiley, New York, NY.

[31] Lehman, J., 2002, "Sequential Design of Computer Experiments for Robust Parameter Design," Ph.D. thesis, The Ohio State Univeristy, Columbus, OH.

[32] Rasmussen, C. E., 1996, "Evaluation of Gaussian Processes and Other Methods for Non-Linear Regression," Ph.D. thesis, University of Toronto, Toronto, ON.

[33] Jin, R., Chen, W., and Sudjianto, A., 2004, "Analytical Metamodel-Based Global Sensitivity Analysis and Uncertainty Propogation for Robust Design," SAE Transactions Journal of Materials and Manufacturing (Paper no. 2004-01-0429).

[34] Xiong, Y., Chen, W., Apley, D., and Ding, X., 2007, "A Non-Stationary Covariance-Based Kriging Method for Metamodelling in Engineering Design," International Journal for Numerical Methods in Engineering, 71(6), pp. 733-756.

[35] Gramacy, R., and Lee, H., 2008, "Bayesian Treed Gaussian Process Models with an Application to Computer Modeling," Journal of the American Statistical Association, 103(483), pp. 1119-1130.

[36] Cressie, N., 1993, *Statistics for Spatial Data*, *Wiley Series in Probability and Statistcs*, Wiley, New York, NY.

[37] Billingsley, P., 1995, *Probability and Measure*, John Wiley & Sons, Inc., New York, NY.

List of Table Captions

List of Figure Captions

Fig. 1 Objective-oriented sequential sampling.

Fig. 2 (a) Response surface for $y(d,w)$. (b) The robust design objective function for the open box example with $d^* = 1.34$ m and $f(d^*) = \$108.30$.

Fig. 3 Sequential sampling algorithm.

Fig. 4 The first iteration of the sequential sampling algorithm using the open box example.

Fig. 5 Sequential algorithm results for the open box example for (a) the location of d_{min} and $f_{GW}(d_{min})$ and (b) the location of the sequentially added points (numbers indicate i) using the EI and MSE criteria.

Fig. 6 Convergence behavior for the engine piston design example. Note the error bars have been moved right slightly for improved visualization.

Tables

Table 1

d_{N+i} Criterion	w_{N+i} Criterion	d_{min}	$f_{GW}(d_{min})$	$\sigma_F(d_{min})$	$f(d_{min})$
True Surface (d^*)		1.34	--	--	108.30
EI	MSE	1.34	108.23	0.02	108.30
EI	wMSE	1.37	108.46	0.27	108.38
EI	IMSE	1.31	108.02	0.41	108.40
EI	VAR	1.38	108.52	1.62	108.43
PI	MSE	1.35	107.83	0.22	108.31
PI	wMSE	1.35	108.29	0.04	108.32
PI	IMSE	1.33	108.20	0.20	108.30
PI	VAR	1.34	107.85	0.82	108.30
One-shot (IU)		1.33	107.35	1.03	108.36
One-shot (no IU)		1.33	106.57	1.03	108.36

Table 2

Variable	Description	Nominal Value	Range/Distribution
d_1	Skirt Profile (SP)	3	1 to 3
d_2	Pin Offset (PO)	0.9	0.5 to 1.3 mm
d_3	Skirt Length (SL)	23.07	21 to 25 mm
d_4	Skirt Ovality (SO)	2	1 to 3
W_1	Piston-to-bore Clearance (CL)	--	$N(50, (11)^2)$ μm
W_2	Location of Combustion Peak Pressure (LP)	--	$N(14.5, 1^2)$ deg.

Figures

fig1.tif

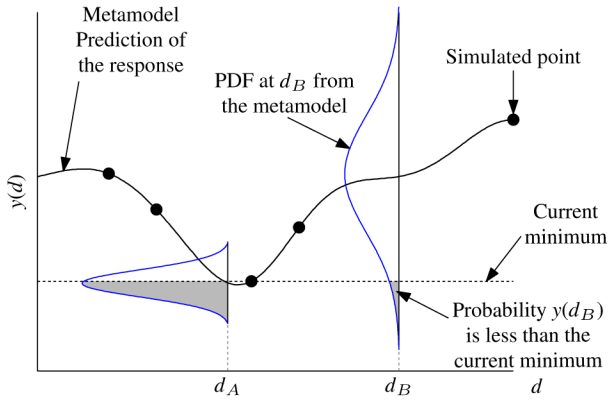

fig2.tif

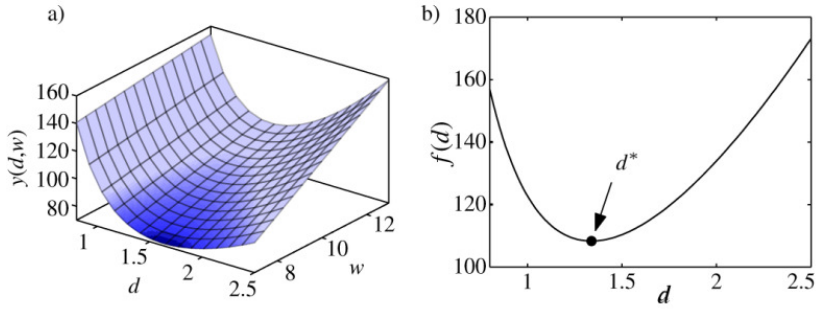
a)
160
140
120
100
80
y(d,w)
1
1.5
2
2.5
d
8
10
12
w
b)
180
160
140
120
100
f(d)
d*
1
1.5
2
2.5
d

fig3.tif

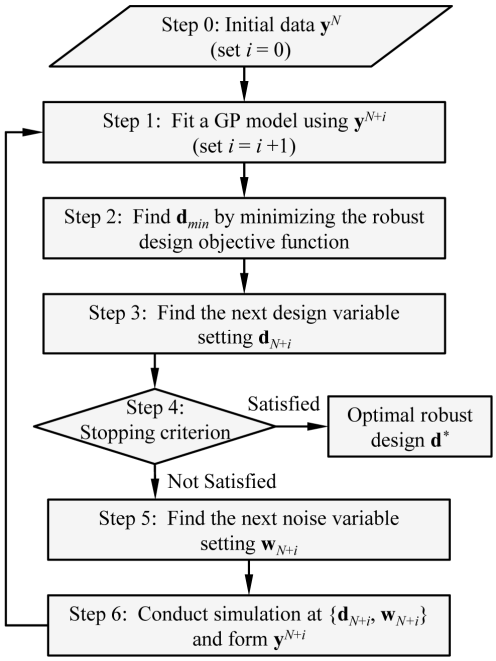
Step 0: Initial data $\mathbf{y}^N$ (set $i = 0$)
Step 1: Fit a GP model using $\mathbf{y}^{N+i}$ (set $i = i + 1$)
Step 2: Find $\mathbf{d}_{min}$ by minimizing the robust design objective function
Step 3: Find the next design variable setting $\mathbf{d}_{N+i}$
Step 4: Stopping criterion
Satisfied
Optimal robust design $\mathbf{d}^*$
Not Satisfied
Step 5: Find the next noise variable setting $\mathbf{w}_{N+i}$
Step 6: Conduct simulation at $\{\mathbf{d}_{N+i}, \mathbf{w}_{N+i}\}$ and form $\mathbf{y}^{N+i}$

fig4.tif

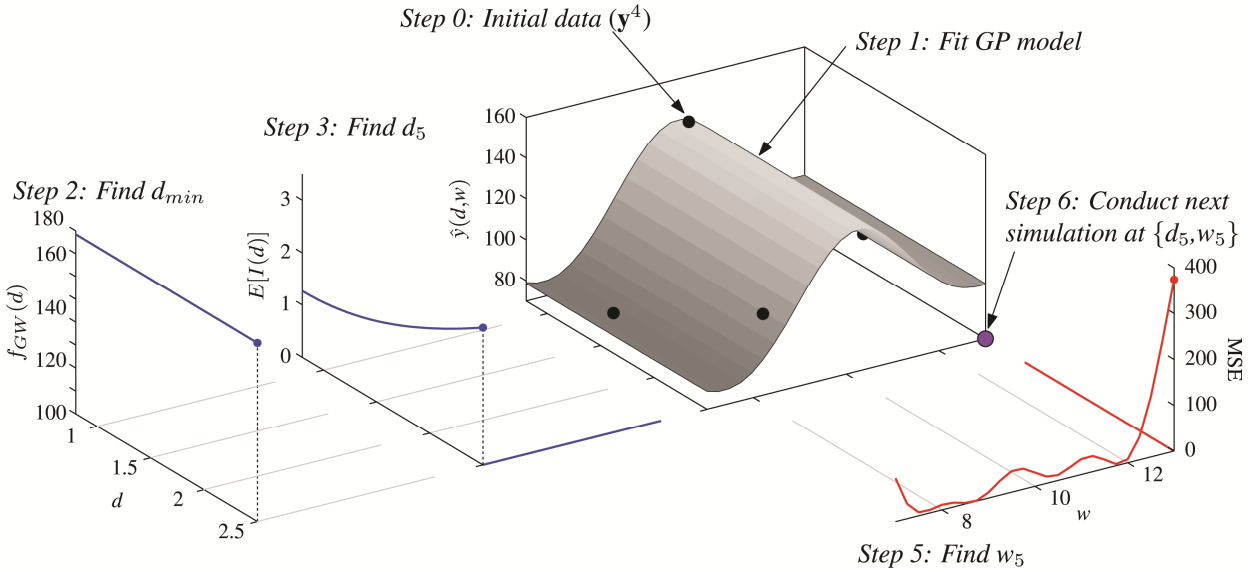
Step 0: Initial data ($\mathbf{y}^4$)
Step 1: Fit GP model
Step 2: Find d_{min}
Step 3: Find d_5
Step 5: Find w_5
Step 6: Conduct next simulation at $\{d_5, w_5\}$
$f_{GW}(d)$
$E[I(d)]$
$\hat{y}(d,w)$
MSE
d
w

fig5.tif

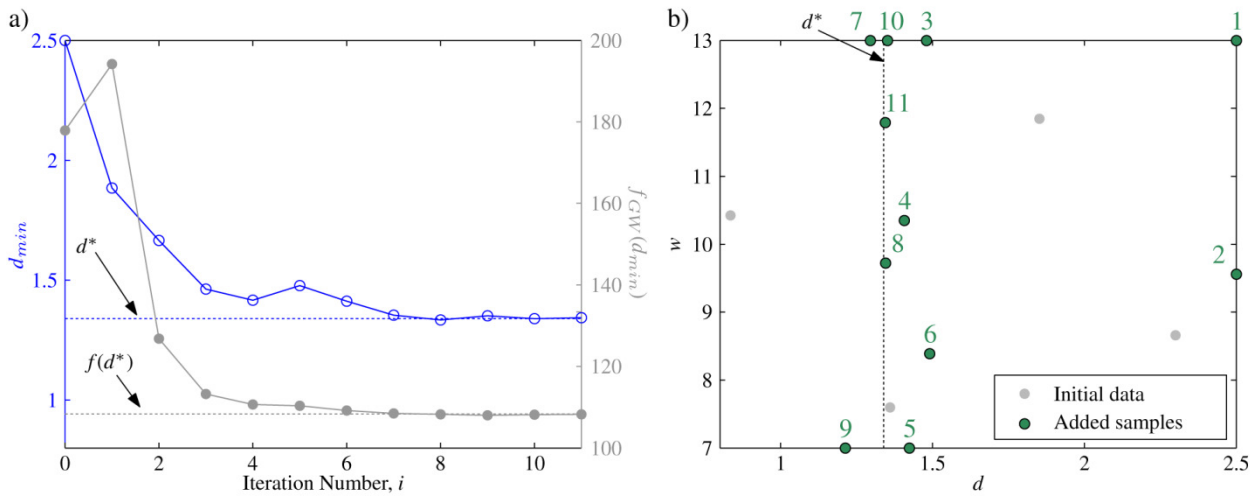
a)
b)
d_{min}
$f_{GW}(d_{min})$
d^*
$f(d^*)$
Iteration Number, i
w
d
Initial data
Added samples

fig6.tif

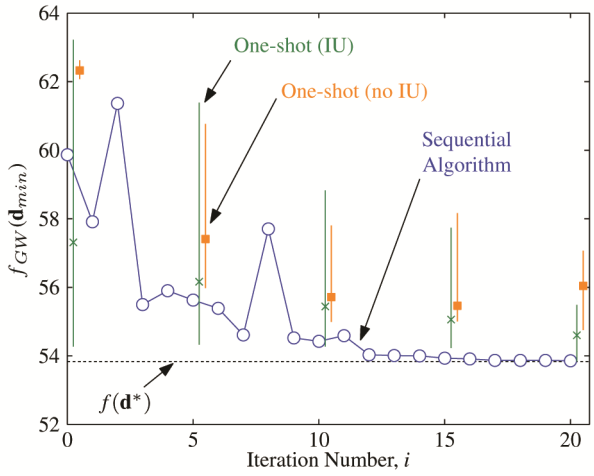
One-shot (IU)
One-shot (no IU)
Sequential
Algorithm
$f(\mathbf{d}^*)$
$f_{GW}(\mathbf{d}_{min})$
Iteration Number, i
64
62
60
58
56
54
52
0
5
10
15
20